energies

MDPI

Article

Development of a Tool for Optimizing Solar and Battery Storage for Container Farming in a Remote Arctic Microgrid

Daniel J. Sambor [1,*], Michelle Wilber [2], Erin Whitney [2] and Mark Z. Jacobson [1]

[1] Department of Civil and Environmental Engineering, Stanford University, Stanford, CA 94305, USA; jacobson@stanford.edu

[2] Alaska Center for Energy and Power, University of Alaska Fairbanks, Fairbanks, AK 99775, USA; mmwilber@alaska.edu (M.W.); erin.whitney@alaska.edu (E.W.)

* Correspondence: dsambor@stanford.edu

Received: 28 August 2020; Accepted: 24 September 2020; Published: 2 October 2020

Abstract: High transportation costs make energy and food expensive in remote communities worldwide, especially in high-latitude Arctic climates. Past attempts to grow food indoors in these remote areas have proven uneconomical due to the need for expensive imported diesel for heating and electricity. This study aims to determine whether solar photovoltaic (PV) electricity can be used affordably to power container farms integrated with a remote Arctic community microgrid. A mixed-integer linear optimization model (FEWMORE: Food–Energy–Water Microgrid Optimization with Renewable Energy) has been developed to minimize the capital and maintenance costs of installing solar photovoltaics (PV) plus electricity storage and the operational costs of purchasing electricity from the community microgrid to power a container farm. FEWMORE expands upon previous models by simulating demand-side management of container farm loads. Its results are compared with those of another model (HOMER) for a test case. FEWMORE determined that 17 kW of solar PV was optimal to power the farm loads, resulting in a total annual cost decline of ~14% compared with a container farm currently operating in the Yukon. Managing specific loads appropriately can reduce total costs by ~18%. Thus, even in an Arctic climate, where the solar PV system supplies only ~7% of total load during the winter and ~25% of the load during the entire year, investing in solar PV reduces costs.

Keywords: microgrid; container farm; solar photovoltaics (PV); renewable energy; storage

1. Introduction

Remote communities in Alaska pay some of the highest prices for electricity in the United States, often in excess of $1/kWh [1]. These high costs are due to the communities' isolation from Alaska's electric grid and its road system. Communities must instead operate and maintain their own diesel generators to provide electricity via a self-contained electric grid, also known as an islanded microgrid. Diesel fuel must be imported over a long distance by plane or boat. Electricity is subsidized for residential use in many communities, but subsidies are not available for commercial operations including for agriculture [1].

Alaskan remote communities are therefore more similar to energy-insecure areas worldwide than they are to the rest of the United States [2]. Most people worldwide facing energy insecurity live in rural areas. For over 70% of them, microgrids provide the best solution to addressing energy insecurity due to the logistical challenges of extending a centralized grid [2,3]. Microgrids can also help to reduce climate change damage, air pollution, and land degradation [4].

Harnessing solar energy for electricity may provide an opportunity to reduce energy costs while increasing reliability and decreasing maintenance costs. A third of Alaska's ~200 microgrids already have some renewable electricity generators installed [1]. However, renewable electricity systems such as solar photovoltaic (PV) arrays require substantial upfront capital investment. Diesel generators have a lower capital cost but a continuous fuel cost throughout their lifetimes. Thus, in order to make solar PV economically advantageous over a diesel generator, the size of the PV system should be optimized and its output should be used as much as possible.

Solar PV electricity generation is also intermittent diurnally and seasonally, especially at high latitudes. In order to provide stable, or firm, electricity production from renewables, battery storage is often installed to balance times of both excess and low PV supply. However, batteries also require substantial capital investment, especially in remote areas. A potentially more cost-effective method of integrating renewable electricity involves scheduling electric loads to operate at higher levels, or even exclusively, during times of otherwise excess renewable electricity output [5]. These methods, including demand flexibility and demand response, are collectively known as demand-side management (DSM) strategies [6,7].

Analogous to energy, food is also expensive in remote Alaskan villages given the high cost of freight by barge or plane. Food prices may be 2.5 times higher in rural Alaska than in cities in the contiguous U.S. and sometimes up to 10 times higher [8]. Indigenous communities have used subsistence practices to harvest meat and plants locally for millennia; however, there has been an increased reliance on market food imports in recent decades, partly due to declining harvests threatened by climate change [8]. Given the lengthy and difficult supply chains, most imported foods are processed and shelf-stable, resulting in a lack of access to quality produce. Some communities have begun gardening in outdoor beds or greenhouses to complement subsistence diets and expensive imports. However, the growing season is short and even greenhouses cannot extend the season through a cold Arctic winter. This limits the ability to grow food with a sufficient number of calories, and most food grown, such as herbs and greens, is used only as nutrients or flavor supplements.

There is an increased interest in container farming in the Arctic in order to grow more food locally, more intensively, and year-round [9]. Given constraints on hydroponic growing, production is generally limited to basil and lettuce. Test-case container farms have demonstrated yields equivalent to an acre of farmland in less than 1% of the area, or in 15% of the area of a typical greenhouse [10]. To grow food more intensively, however, significant energy is used by container farms, leading to expensive operational costs. Therefore, while container farms may provide additional time over a year to grow food and more concentrated means of doing so, their effectiveness in affordably addressing food security is still an open question.

Using local renewable electricity generation may reduce the energy cost of container farms. However, there are challenges in properly balancing and integrating intermittent renewable electricity sources, such as solar PV, with container farming. The focus in this study is to optimize the nameplate capacities and operations of solar PV, batteries, and farm loads when all are connected to the community microgrid.

Controlled environmental agriculture (CEA), of which container farming is a subset, has been noted for its potential to flexibly adopt loads to integrate renewable energy, however, no study has specifically analyzed such a prospect [11]. Studies have analyzed how to best retrofit a container farm with the optimal growing equipment, but have assumed fixed energy requirements of plants without the ability to incorporate DSM [12,13]. For example, DSM of specific farm electric loads, such as lighting, ventilation, and dehumidification, can allow for optimal demand dispatch coincident with available solar energy. This can reduce cycling of a battery system, all while maintaining indoor plant growing constraints.

There are numerous computer models in the literature for optimizing renewable energy systems around a specific load within a microgrid [14,15]. There is generally a tradeoff between computational speed and model complexity. Mixed-integer linear programming (MILP) methods have often been

used, given their ability to solve problems at speed with necessary detail, as state-of-the-art in energy system modeling [16].

Commercial tools have been built to bridge this gap of complexity and performance with speed and accessibility in designing renewable energy microgrids. For example, the default tool for analyzing microgrids is HOMER (Hybrid Optimization of Multiple Energy Resources), originally developed at the National Renewable Energy Laboratory (NREL). HOMER has been used widely for modeling remote islanded microgrid systems [17]. Singh et al. [18] compares the hybrid PV–wind–biomass–storage optimization in HOMER with an evolutionary algorithm approach, which has better performance. Shoeb and Shafiullah [19] use HOMER to optimize operation of water pumps in a microgrid with solar PV. Tapia [20] implemented a HOMER model to study hybrid renewable energy optimization of a container farm; however, the load profile was assumed fixed and no load flexibility was implemented in this analysis.

Still, other microgrid design tools have been developed by government labs and organizations. NREL has developed ReOpt (Renewable Energy Integration and Optimization) Lite as an open-source tool for optimizing solar and storage capacity for a specific load, and is based on the more complex ReOpt software; however, it is not possible to manipulate the load profile to analyze DSM of specific loads [21]. NREL has also developed RPM (Resource Planning Model) to analyze the value of flexibility of battery storage and interruptible loads, but it is used at a large-scale for capacity expansion modeling [22].

Numerous microgrid models have also been developed that use demand-side management. Neves et al. compare a self-built economic dispatch model that uses genetic algorithms with the capabilities of HOMER for modeling demand response [23]. They emphasize that there is a significant challenge in using commercial tools for demand response modeling and have found that most models using DSM are self-built. An optimization framework must also balance long-term investment planning with short-term dispatch strategies [24]. HOMER cannot schedule specific loads as part of an overall demand profile in hourly increments with custom dispatch strategies, and instead distributes flexible load operations evenly across a day [23].

A model has not yet been developed that optimizes the capacity and dispatch of novel food–energy–water controllable loads for demand-side management as part of a container farm in islanded renewable microgrids. Most models also do not account for thermal energy requirements or optimization, which is more typically suited for energy models for buildings. Numerical models for operating container farms have been developed, though these do not include energy optimization strategies with renewable energy systems [25]. Other tools have been designed around the food–energy–water nexus, but optimize the size of a greenhouse—not a container farm or individual loads—with a solar PV array [26].

This paper's contribution, then, is the development of a tool, FEWMORE: Food–Energy–Water Microgrid Optimization with Renewable Energy, to optimize the capacity and operations of a solar PV and battery system in order to power optimally-scheduled loads of a container farm within a remote islanded microgrid. Additionally, for modeling flexible loads, it is critical to have a tool tailored to specific constraints and system dynamics of which no energy optimization model is currently articulated for container farms. The model also balances electric and thermal (both sensible and latent) energy requirements.

The rest of the paper is structured around container farming description, modeling methodology, and energy simulation results and conclusions.

2. Container Farming

Container farms have been introduced in the Arctic due to their modular nature, ease of transport and siting, and ability to grow food year-round indoors in a well-insulated unit [27]. Shipping containers are already a relatively common method of transporting goods to Alaskan villages. These containers are generally retrofitted with hydroponic growing systems, in which plants are grown in trays of

circulated nutrient-rich water. In addition to being highly productive, this system does not use soil, which can be advantageous in Arctic areas without access to fertile soil [28]. An example of a container farm is a CropBox unit, which can produce 5400 kg (12,000 lbs) per year of herbs and greens [10]. Based on an analysis of a CropBox, the cost of growing this produce (in a typical location) is $6.34/kg ($2.88/lb) including all energy, labor, and miscellaneous costs [12].

Table 1 provides the typical characteristics of a hydroponic growing container used for this analysis [29]. All heating, ventilation, and air-conditioning (HVAC) are assumed to be electric. There are also accessory loads including those for carbon dioxide (CO_2) pumping, nutrient pumping, and sensors that have negligible electric requirements, and therefore are not included. The loads are assumed to be well optimized in size within an energy-efficient container.

Table 1. Electric loads, capacity, and operation description of the container farm assumed for this study.

Load	Power (W)	Duration
Air Circulation Fans	220	Always On
Water Pumps	720	Always On
Lighting	4500	18 h/day
Heating/Cooling	2000	As needed to maintain 20 °C
Ventilation/Exhaust Fan	110	As needed
Dehumidification	1500	As needed to maintain 65–75% relative humidity

Loads that are on at all times or baseloads include air circulation fans and water pumps for the hydroponic growing trays. These total approximately 1 kW of instantaneous power. They can, in theory, be shut off for a period if there is a lack of renewable power; however, in reality, this may lead to a decline in produce quality, so were not considered for the DSM. All equipment results in heat gain, which must be removed via cooling if the unit exceeds its interior temperature range.

Due to its opaque envelope, a container farm substitutes natural sunlight with LED grow lights at a relatively high energy demand. LED arrays provide lighting for 18 h per day at 4.5 kW (or 81 kWh per day). While LED lighting is relatively efficient, this still implies that nearly all of the 4.5 kW of electricity is dissipated as heat to the indoor environment, leading to a potentially high cooling load. Lights are assumed to operate continuously during the 18-h block, but can be scheduled to be on during any time of day.

Dehumidification is also a significant load. Plants transpire, resulting in an accumulation of humidity in the indoor space, or latent heating load. Plants also reduce the sensible heat load due to the evaporative cooling effect of evapotranspiration, thus offsetting some heat gains from lighting and other equipment. These effects occur primarily during lighting hours; it was assumed that the ratio of transpiration during the plants' day to night was 3:1 [30]. The container farm operates at an optimal 65–75% relative humidity (RH); we assumed the RH was fixed at 70% [29]. If this level is exceeded and moisture is not removed, then fungal growth and disease may occur; alternatively, if too much moisture is removed, plants may desiccate and reduce yield. A dehumidifier, rated at 1.5 kW, was assumed to operate continuously during the baseline operation of a container farm [31] (See Appendix C.3. for additional energy modeling detail). However, this load may be dispatched accordingly, as long as the RH is managed using ventilation.

Ventilation can be used, especially in an Arctic climate to balance sensible and latent thermal loads by exhausting warm, moist indoor air and replacing it with cold, dry ambient air, respectively. The cost of carbon dioxide pumping must also be accounted for when considering ventilation, given that plants have higher yields at elevated CO_2 levels and excessive ventilation would increase costs due to the high price of replacing compressed CO_2 [32]. However, during winter, when there is significant potential to use ventilation for cooling due to the high temperature and humidity difference between the indoor and ambient air, no CO_2 pumping is used given the reliance on outdoor air exchanges in the baseline operation. There is also a minimum number of continuous air exchanges in the container farm,

assumed to be 0.5 air changes per hour, due to the combined effects of infiltration and ventilation [33] (See Appendix C.2).

Heating and cooling are provided via an electric fan-coil unit. This unit cycles throughout the day and requires ~2 kW. In the baseline case, it is assumed to operate for half the time in a given day (See Appendix A for technology modeling parameters). Thermal energy flows include sensible and latent heat balances. During the vast majority of a year in the Arctic, the ambient temperature is colder outside than the balance point temperature set by the thermostat (20 °C). Sensible heat loss occurs via conduction through the container envelope, infiltration, and ventilation of outside air, and evaporative cooling from plants. Sensible heat gains result from mechanical equipment, and from exterior conduction and infiltration on warm summer days (See Appendix C.1). Latent heat must also be balanced due to the plants' emitted moisture as well as the latent component of infiltration and ventilation air flows (See Appendix C.3).

3. Methods

The FEWMORE model is applied to a community in Interior Alaska that is interested in local food production and renewable energy, and does not currently have a container farm. This analysis uses collected data from an operating CropBox container farm in Whitehorse, Yukon. These data are used within the FEWMORE model to analyze a control case, named the Base Case, of optimizing solar PV and battery storage with container farm loads in the status quo. Then, the FEWMORE model is used to optimize solar and storage while allowing the prior container farm load profile to be flexible and optimally dispatched, named the Dispatchability Case. In this section, the collected data are analyzed, the FEWMORE model is summarized, and a model simulation procedure is presented.

3.1. Container Farm Load Data

A year of power consumption data was collected for the CropBox unit operating in Whitehorse, Yukon, Canada. The data contains the total energy consumption values at 5-min temporal resolution from November 2018 to October 2019, which have been processed to align with a calendar year and averaged to hourly resolution. Averaged diurnal load profiles for each season are shown in Figure 1.

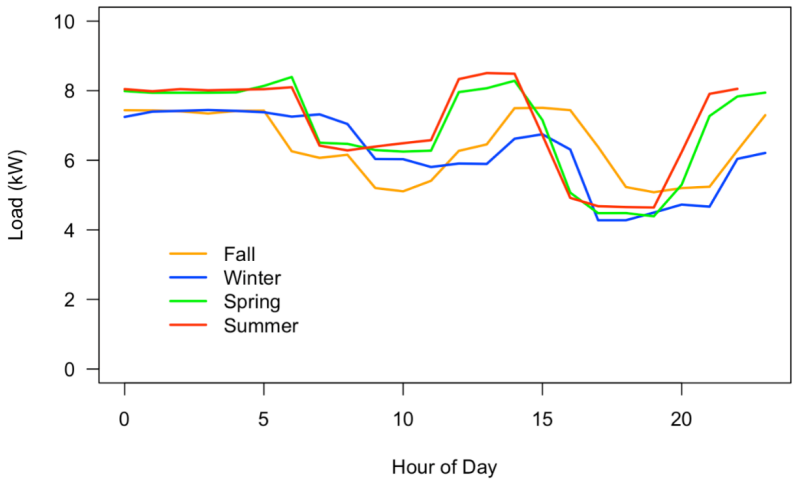

Figure 1. Averaged hourly electric daily load profiles of a container farm in Whitehorse, Yukon for fall (September–November), winter (December–February), spring (March–May), and summer (June–August). Electricity use is greatest overnight along with a midday peak when all loads (lighting, heating/cooling/ventilation, dehumidification) are operating. Reductions in electric use occur in the mid-morning hours, which can be attributed to reduced heating, cooling, and dehumidification as well as late afternoon and evening hours when lighting is turned off. Summer electricity use is generally highest, given substantial cooling required to exhaust waste heat from operating electric loads, which are nearly sufficient to heat the opaque container in the winter.

Electricity use in the container farm follows a relatively similar daily profile from season to season. Consumption is fairly constant over a day, peaking at 8 kW when all loads are operating, typically overnight and in the middle of the day. During the late afternoon and early evening, approximately 3 pm–9 pm, lighting is shut off. In the mid-morning hours, there is also a reduction in energy use due to less HVAC and dehumidification operation. The profile is slightly shifted later in the day during the fall and winter, presumably due to daylight savings time and later sunrises. In November 2018, during system initialization, there was slightly less energy use, with a peak power demand of 6.5 kW.

3.2. Model Summary

The FEWMORE model is a mixed-integer linear program built in the Julia/JuMP optimization language. The modeling framework has been chosen to reduce computational expense while preserving necessary modeling complexity. Optimization is performed hourly for energy operations and DSM, over an annual capacity planning horizon. The single-year output was extrapolated with perfect foresight to a 20-year project lifetime, subject to a discounted cash flow analysis. The FEWMORE model output was also ultimately compared with HOMER.

The objective of FEWMORE is to minimize the total net present cost of the project, namely capital and lifetime operational costs of powering a container farm (See Appendix B for model form detail). The final objective cost is also divided by the total amount of greens grown over the lifetime to estimate an energy cost per unit of crop production. Assuming the container itself is already purchased, the total project cost includes purchasing, installing, and maintaining the solar PV, battery storage, and power conversion infrastructure to couple directly with the container, in addition to buying electricity from the community microgrid. Grid electricity is purchased at an unsubsidized rate of $0.67/kWh, and prices are assumed to escalate annually at a real rate of 3% [34]. Capital costs include the solar array, with a 20-year lifetime, and a battery and inverter with a 10-year lifetime, replaced at a real discount rate of 3%. Operational costs include a solar PV maintenance cost of $50/kW/yr and a variable cost of battery system maintenance of 0.5 cents per kWh throughput.

The model inputs included the container farm electric load profile and solar yield profile. To determine a synthetic thermal load profile, the ambient temperature and humidity were also used for the specific Interior Alaska climate. The model output the optimal capacity of additional infrastructure (solar PV, battery storage, and inverter) as well as an hourly dispatch of all technologies (battery charging/discharging and DSM of select loads) (See Appendix A for all model inputs and outputs). The dispatch of flexible loads including ventilation fans and dehumidifiers were constrained by physical requirements and optimized for lowest operating cost (See Appendix B).

3.3. List of Model Simulation Cases

Two sets of simulations were performed, one with the collected electric load data named the Base Case, and the other with a flexible, synthetic electric load profile known as the Dispatchability Case, as shown in Table 2. The synthetic load profile was derived from typical patterns in the collected electric load data in order to disaggregate specific loads and optimally dispatch them as part of DSM strategies. Lighting was fixed in the synthetic profile to operate coincident with the solar noon. The synthetic load profile also included a sensible heat and latent heat thermal load profile, derived from profiles of ambient temperature and ambient humidity, respectively, to model the optimal operation of the HVAC and dehumidifier units.

Table 2. Outline of model simulations performed for the two cases studied: Base Case, using load data collected from an operating containers farm; and Dispatchability Case, using a synthetic load profile based on optimization of dispatchable loads with demand-side management strategies.

Base Case:	Dispatchability Case:	Model Notes
Collected Load Profile	**Synthetic Load Profile**	
Baseline	Baseline	Only grid electricity is used (no optimization is performed)
Solar	Solar	Amount of solar capacity optimized
Solar & Storage	Solar & Storage	Amount of solar and battery/inverter capacity optimized
Lighting with Solar	-	Lighting is shifted to be symmetric around solar noon for Collected Load Profile and only solar is optimized
Lighting with Solar & Storage	-	Same as above, except both solar and storage are optimized
-	Ventilation	The number of air changes per hour (ACH) ventilated to provide cooling/dehumidification is optimized, and the amount of solar and storage is optimized
-	Dehumidification	Same as Ventilation simulation, except the operation of the dehumidifier (on/off) is also optimized

For each of the two sets of simulation cases, the Base Case and Dispatchability Case, the same three simulations were initially performed. The first simulation (named Baseline simulation) analyzed the container farm operations when all loads were powered by the community microgrid at the unsubsidized electricity rate. In the next simulation (Solar simulation), the amount of solar PV capacity to be added to the container farm was optimized. The solar array generated electricity to be used directly by the container farm, thus potentially reducing the amount of energy purchased from the microgrid, and any excess solar generation beyond the farm load was curtailed. In the Solar & Storage simulation, the amount of battery storage capacity and inverter power capacity were optimized including hourly charging and discharging strategies, in addition to solar PV optimization.

The next simulations (Lighting with Solar, and Lighting with Solar & Storage) were performed only for the Base Case. The lighting schedule was modified from the collected load data, which included lighting operating for an 18-h block somewhat parallel with solar daylight hours (approximately two hours misaligned from solar noon), to a schedule that was perfectly centered around peak solar PV output. The rest of the load profile was assumed to be the same. Then, solar PV capacity and solar PV plus battery storage capacities were optimized for the two respective cases.

The final simulations were performed only for the Dispatchability Case, using a synthetic load profile to analyze DSM strategies of specific loads. The first simulation, named Ventilation, optimized the operation of the ventilation system by determining the number of air changes per hour to perform, given constraints on replacing CO_2 and thermal load requirements. The next simulation, named Dehumidification, optimized how the dehumidifier should operate, in addition to the ventilation system. The dehumidifier was optimized to turn on and off, given that it was assumed to run at a single maximum power setting when operating.

4. Results and Discussion

The results of the model simulations outlined in Table 2 are presented first for the Base Case (Section 4.1), with the collected load profile, and second for the Dispatchability Case (Section 4.2), with the synthetically derived load profile.

4.1. Base Case Simulations

4.1.1. Baseline Simulation

In the baseline simulation, all energy use, or 58.4 MWh per year, was met by purchases from the diesel powerhouse of the community microgrid. The energy cost of operating the farm was $39 k per year, or $783 k for the entire 20-year lifetime. Dividing by the total production of greens over the lifetime resulted in an energy cost per unit of crop produced of $7.17/kg ($3.26/lb).

4.1.2. Solar and Storage Simulations

The model determined that the optimal nameplate capacity of solar PV alone (Solar simulation) to be added to the container farm was 17.1 kW. The solar capacity was approximately 33% higher than the container farm's peak load of 12.8 kW. The total solar electric energy generated was 18.9 MWh/yr, of which 4.8 MWh (~25%) was curtailed (no battery storage is assumed for this simulation). The overall project cost decreased by $106 k compared with the baseline case, or a 13.5% reduction due to adding solar PV. The energy cost of crop production was $6.20/kg ($2.82/lb).

In the Solar & Storage simulation, a battery storage system was added and optimized for its energy capacity and inverter power. The model added a very small battery system of 1.2 kWh/0.5 kW of energy and power capacity, respectively; thus, the total objective cost was nearly the same as in the solar PV-only simulation. The optimal solar PV capacity was 17.5 kW and a total solar electric energy generation of 19.4 MWh/yr with 4.9 MWh curtailed. Similar to the Solar simulation, the energy cost per unit of crop production was $6.20/kg. The battery was used to extend the solar day slightly as shown in Figure 2, in which some excess solar energy was used to charge the battery in the early morning and late afternoon, and then was discharged in the early evening once solar PV output had declined below the container farm load. The vast majority of excess solar energy was otherwise curtailed.

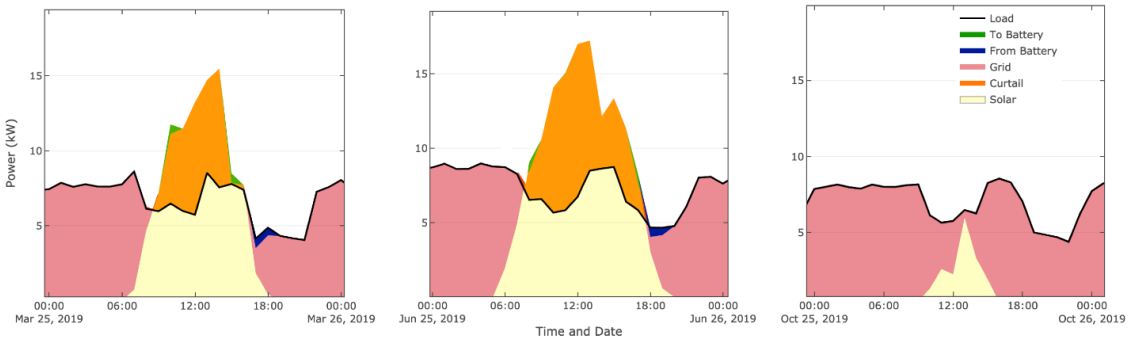

(**a**) (**b**) (**c**)

Figure 2. Modeled electric profiles resulting from operating the optimized solar and storage system with the collected container farm load data for three representative seasonal periods: (**a**) spring, (**b**) summer, and (**c**) fall. In spring, a small amount of excess solar was used to charge the battery at the beginning and end of the solar day with even smaller amounts of charging necessary during the summer, given that more solar energy is available from day to day. Any excess solar generation, beyond the load and charging to the battery, was curtailed. When the battery had energy in storage, it was fully discharged in the early evening hours. In late fall and winter, solar energy output was less than the container farm load.

As shown in Figure 2, given the small size of the recommended battery capacity, it did not provide substantial benefit to the system in terms of dispatching energy. The 0.5 kW rated power of the battery is only about 6% of the farm's peak load. Given 1.2 kWh of storage capacity and discharged at the maximum rate of 0.5 kW, the battery can provide 6% of load for 2.4 h. Thus, while the solar array could meet the container farm load for approximately half of a day during spring and

summer, the battery system offered comparatively negligible autonomy. Over the course of a year, only 1.5% of solar generation was used to charge the battery. The low utilization of battery optimization by FEWMORE can be attributed to the relatively high battery storage and power conversion costs ($1000/kWh, $1000/kW) assumed for the Interior Alaska region; in less remote areas with lower costs, the battery capacity may increase.

The solar PV array, with the small battery energy storage system, provided 25% of the power needs of the container farm over the course of the entire year, as shown in Figure 3. Electricity from the solar array met the load first and any excess was stored or curtailed. In the winter, only 7% of load was met by solar plus storage, with the rest provided by purchases from the community microgrid and its diesel powerhouse. In the summer months (June through August), 38% of load was met by renewable energy. Spring (March through May) resulted in a similar amount of renewable energy penetration compared to summer, as relatively high sun angles and reflectance from snow cover can lead to improved solar performance.

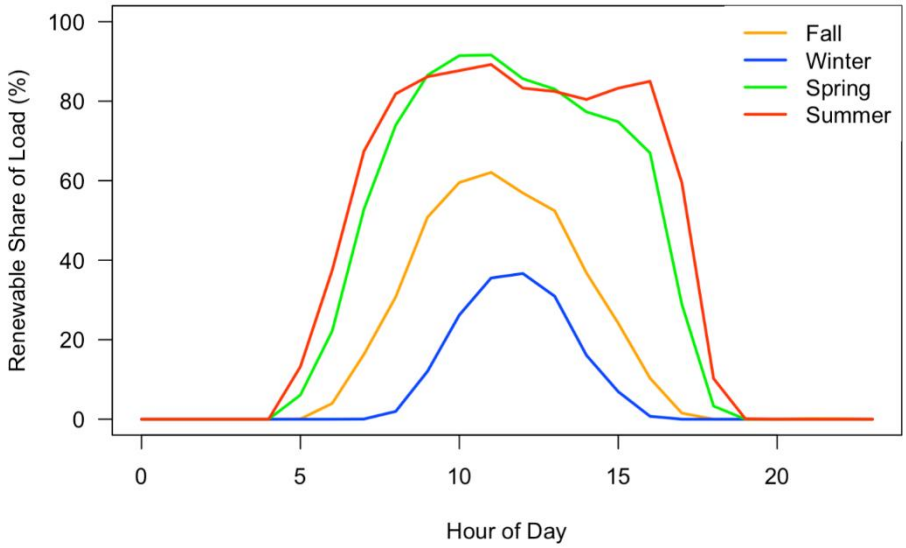

Figure 3. Amount of load met by solar and storage in each hour of the year. Only 7% of load was met by the renewable energy system in the winter months, and the rest was provided by community microgrid purchases. In the summer months, 38% of load was met by solar plus storage.

4.1.3. Lighting Simulations

Two simulations were performed in which the lighting schedule in the collected load profile was modified to be perfectly symmetric around the solar PV generation peak output. Originally in the collected electric load profile, lighting did not operate during late afternoon and early evening hours. The Lighting with Solar and Lighting with Solar & Storage simulations were performed for the optimization of solar PV and solar PV plus battery energy storage, respectively. However, given the results for the solar PV-only and solar PV-plus-battery energy storage simulations were quite similar, only results with respect to the solar PV-only (Lighting with Solar) simulation are presented.

The optimal solar PV array power capacity increased marginally from 17.1 to 17.3 kW when the lighting schedule was modified to be symmetric around solar noon in the Lighting with Solar simulation. Thus, the collected data profile was already relatively optimal, given lighting was scheduled for most of the peak solar PV generation hours, approximately 10 am–4 pm. Solar PV power capacity increased, albeit slightly, given the larger amount of load coincident with solar hours. The energy cost of crop production declined marginally by two cents per kilogram from $6.20/kg to $6.18/kg because a larger percentage of the load was met directly by solar PV.

The simulations using FEWMORE in Sections 4.1.1–4.1.3 were repeated using HOMER, with the results displayed in Table 3 for comparison. The HOMER model was developed using the same

assumptions as the FEWMORE model. The total cost objectives varied ~4–7% between the two models. The HOMER model resulted in an energy cost per unit of crop production of $6.64/kg ($3.02/lb) for the Solar simulation.

Table 3. Summary of results using the FEWMORE (Food-Energy-Water Microgrid Optimization with Renewable Energy) Model compared with HOMER for simulations, using the collected container farm data (*Base Case*). Total cost objectives were ~4–7% higher and solar capacities were ~9% lower in HOMER compared to FEWMORE.

Model	**FEWMORE**				**HOMER**			
Simulation Name	**Baseline**	**Solar**	**Storage**	**Lighting**	**Baseline**	**Solar**	**Storage**	**Lighting**
Total Cost (k$)	783.3	675.1	675	674.9	783.4	725	725.7	710.4
Produce Cost ($/kg)	$7.17	$6.20	$6.20	$6.18	$7.17	$6.64	$6.64	$6.51
Grid Energy (MWh/yr)	58.4	44.3	44	44.2	58.4	47.7	47.6	46.5
Solar (kW)	-	17.1	17.5	17.3	-	15.6	15.6	15.8
Storage (kWh)	-	-	1.2	-	-	-	1	-
Inverter (kW)	-	-	0.5	-	-	-	0.66	-

HOMER recommended a smaller solar array of ~1.5–2 kW generally across the simulations compared to the FEWMORE model. While this was a ~9% difference in solar capacity compared to FEWMORE in the Solar simulation, the resulting changes in total objective cost were smaller. For example, if the HOMER results for solar capacities are given to the FEWMORE model as fixed inputs, the objective cost of the FEWMORE model changes by less than 0.1% compared to the optimal FEWMORE solar capacity. Thus, differences in solar capacity have less of an effect than other parameters, as highlighted in Section 4.1.4.

4.1.4. Sensitivity Analysis for FEWMORE Solar Simulation

A sensitivity analysis was performed around certain parameters for the Solar simulation using FEWMORE. The energy cost per unit of crop production of $6.20/kg in Table 3 resulted from the model assumptions of a 3% real discount rate and 3% escalation rate (accounted for inflation). Instead, varying the escalation rate from 1–5% (with a fixed discount rate at 3%) resulted in costs of $5.21 to $7.39/kg ($2.37–$3.36/lb) and solar capacity of 14.2 kW to 25.7 kW. For a fixed escalation rate of 3%, varying the discount rate from 2–6% resulted in costs of $6.80 to $4.82/kg ($3.09–$2.19/lb) and solar capacity from 18.9 kW to 13.5 kW.

Thus, the financial parameters of investing in container farm energy infrastructure may have a relatively substantial effect on optimal infrastructure sizing within the FEWMORE model. Reducing the discount rate by one percent increased the size of the solar array by 2 kW (~11%), and increasing the grid escalation rate by one percent increased the solar PV array size by 6 kW (~35%). A sensitivity analysis with respect to solar capital expenditure ($/kW), solar operating expenditure ($/kW/yr), battery energy storage capital cost ($/kWh), and inverter capital cost ($/kW) resulted in comparatively insubstantial changes compared to the sensitivity analysis on discount and grid escalation rates.

4.2. Dispatchability Case

Compared to the Base Case, which used collected electric load profile, simulations in the Dispatchability Case were performed using a synthetically-derived profile of electric and thermal loads. The purpose of this study was to determine if the operations of the HVAC and dehumidification loads could be optimized to reduce costs and improve energy flexibility, while maintaining temperature and humidity constraints on plant growth.

4.2.1. Baseline Simulation

The FEWMORE model was modified slightly for use of a flexible, synthetic electric load profile. Beginning with the Baseline simulation, the model had the following collective assumptions: baseloads

were always on; fixed heat gains from dehumidification and lighting were constant; lighting was symmetric around solar noon; no ventilation was optimized aside from fixed minimum ventilation and infiltration; and the dehumidifier was always on to meet the latent heating load. The HVAC system operation was optimized and must heat if there is a net heat loss, and cool if there is a net heat gain in each time step.

The baseline for the synthetic profile resulted in an energy cost of crop production of $7.55/kg ($3.43/lb), with the full results displayed in Table 4. This was about 5% higher than the collected profile baseline, given that the synthetic load profile used about 6% more energy than the baseline profile. A notable insight of the model was that no hours of heating were required, given substantial heat gain from mechanical equipment, especially that of the dehumidifier.

Table 4. Summary of results using a synthetic load profile in the FEWMORE model to analyze dispatchability of ventilation and dehumidification systems. Optimizing the dispatch of the ventilation system, in addition to adding a solar array, reduced costs by ~18%. Managing the demand of the dehumidification system, in addition to the ventilation system, did not provide any benefit.

	Simulation Name			
Output	**Base**	**Solar**	**Ventilation**	**Dehumidification**
Total Cost (k$)	824	706	674	678
Produce Cost ($/kg)	$7.55	$6.47	$6.18	$6.23
Grid Energy (MWh/yr)	62.4	44.8	42.5	42.8
Cooling Energy (MWh/yr)	11.4	11.4	9	9.2
Heating Energy (MWh/yr)	0	0	0	0.5
Solar (kW)	-	21.5	21.3	21.4
Storage (kWh)	-	-	0	0
Inverter (kW)	-	-	0	0

4.2.2. Solar and Storage Simulations

Compared to the Baseline simulation, optimizing solar PV alone (Solar simulation) led to a 21.5 kW array and a 15% decrease in cost, as shown in Table 4. The energy cost per unit of crop production was $6.47/kg ($2.94/lb). Even with the option to add battery energy storage (Solar & Storage simulation), the model did not optimize for storage; thus, this result was not displayed. Therefore, solar PV alone was optimal given that most of the electric load (primarily lighting) occured during daytime hours.

4.2.3. Demand-Side Management (DSM)

Ventilating excess heat optimally may allow for a more cost-effective method of operating the container farm. Ventilation may be used for cooling during most of the year, given there are only 178 h of the year during which the ambient temperature exceeds 20 °C in northern Alaska. In the Ventilation simulation, the model optimized when to ventilate and the number of air changes per hour (ACH) to perform. Thus, the cooling system was allowed to turn off to some extent, compared to the Baseline simulation, assuming the same sensible and latent thermal load profiles. The dehumidifier was assumed to operate at all times at its full power capacity, in order to examine the effects of adding only one dispatchable load at a time (the ventilation exhaust fan first). The dehumidifier could modify its moisture removal rate from 30–100% of its rated specification while maintaining the same power draw [31].

The results of using ventilation as a dispatchable load are shown in the Ventilation simulation in Table 4. Overall cost declined by 4.5% compared to the Solar simulation, with a $6.18/kg ($2.81/lb) energy cost. The optimal solar array size was slightly smaller at 21.3 kW and no storage system was recommended. Given no utilization of CO_2 during winter was allowed, and thus no subsequent pumping cost compared to the rest of the year, ventilation was performed exclusively during winter.

The model optimized for ventilation to occur at greater rates during times of high demand for cooling and also when the ambient temperature was only modestly cold (>0 °C).

In the final simulation (Dehumidification in Table 4), the dehumidifier was optimized to turn on and off to minimize energy costs while maintaining sensible and latent thermal energy balance. Given that a dehumidifier emits a significant amount of heat during operation, when it is off the HVAC system must provide heat to the unit. With the opportunity to optimize dispatch of the dehumidifier, the model chose only to interrupt its operation 3% of the time. This yielded similar results to the prior Ventilation simulation and an energy cost of crop production of $6.23/kg.

Therefore, operating the dehumidifier, which provides sensible heat addition and latent heat removal, is in general preferable to requiring heat addition from the HVAC system and latent heat removal via ventilation of ambient dry air. Dehumidification was turned off primarily during moderately cold weather and very dry ambient air conditions, given that supplemental heating was less necessary during those times and the most benefit of latent heat removal via dry ambient air can be realized.

5. Conclusions

This paper provides an initial planning tool for Arctic communities interested in container farms to understand their overall energy use, as well as strategies to modify them appropriately for islanded renewable microgrids. A tool (FEWMORE) has been developed specifically to optimize container farm loads together with solar and battery nameplate capacities when all three are connected to the existing local microgrid.

Adding approximately 15–17 kW of solar PV nameplate capacity to power the container farm was optimal based on a collected electric load profile of an experimental farm. Battery energy storage did not provide substantial benefits, and is not justified. FEWMORE recommended adding 17.1 kW of solar PV, slightly higher than the optimal result of 15.6 kW from the HOMER model. Using a synthetically-derived load to allow for optimizing demand-side management of loads, namely ventilation fans and a dehumidifier, resulted in reductions in energy cost of up to 18% from the baseline. The subsequent cost of energy delivered per unit of crop production was reduced from $7.55 to $6.18/kg ($3.43–$2.81/lb). Analyzing other forms of energy storage, modeling at a higher temporal resolution, and studying additional integration with a community microgrid, such as modeling benefits in frequency regulation or export of excess energy, are left to future work.

This paper presents an initial modeling framework, and the control strategy and assumptions on container farm operations and specific loads have not been experimentally validated. The study builds on early stages of installing a CropBox container farm at the Kluane Lake Research Station (KLRS) in Yukon Territory, Canada. Future work will utilize the KLRS system year-round for expanded data analysis and experimental operation of the strategies recommended here. There are numerous other demand-side management techniques, such as shifting baseload and thermal storage, that can also be incorporated in the future.

Author Contributions: Conceptualization, D.J.S., M.W., and E.W.; Methodology, D.J.S., M.W., and E.W.; Software, D.J.S.; Validation, D.J.S. and M.W.; Formal analysis, D.J.S., and M.W.; Investigation, D.J.S., and M.W.; Resources, D.J.S., M.W., and E.W.; Data curation, D.J.S., and M.W.; Writing—original draft preparation, D.J.S.; Writing—review and editing, D.J.S., M.W., E.W., and M.Z.J.; Visualization, D.J.S.; Supervision, M.W., E.W., and M.Z.J.; Project administration, E.W.; Funding acquisition, E.W. All authors have read and agreed to the published version of the manuscript.

Funding: This research was funded by the United States National Science Foundation, Award #1740075—"INFEWS/T3: Coupling infrastructure improvements to food-energy-water system dynamics in small cold region communities: MicroFEWs".

Acknowledgments: The authors would like to acknowledge the technical support and data provided by Solvest Corporation as well as general support and advice from the MicroFEWs group and David Denkenberger.

Conflicts of Interest: The authors declare no conflict of interest. The funders had no role in the design of the study; in the collection, analyses, or interpretation of data; in the writing of the manuscript, or in the decision to publish the results.

Appendix A. Model Inputs and Outputs

Appendix A.1. Time Series Inputs

- Electric Load profile (l_t) [kW]
    - Base Case: Collected profile from CropBox operation for one year in Whitehorse, Yukon
    - Dispatchability Case: Synthetic profile disaggregated by load
- Ambient Temperature profile $(T_{amb,t})$ [°C]
- Ambient humidity ratio (RH_t) [kg_{H2O} / kg_{dryair}]
- Solar Yield profile (s_t) [kW_{AC} / kWp_{DC} installed]

Appendix A.2. Economic Inputs

- Grid Price (unsubsidized): C_G = \$0.67/kWh
- Project Lifetime: y = 20 years (for all equipment, except battery storage, which has a 10-year lifetime)
- Real Discount Rate: 3%
- Real Grid Escalation Rate: 3%
- Solar Capacity Cost (installed): C_S = \$4500/kW
- Solar Operation & Maintenance (O&M) Cost: O_S = \$50/kW/yr
- Capacity cost of battery inverter (installed): C_I =\$1000/kW
- Capacity cost of battery storage (installed): C_E =\$1000/kWh
- Battery O&M Cost: \$0.005/$kWh_{throughput}$

Appendix A.3. Technology Inputs

- Battery Round-Trip Efficiency: 90%
- Battery Depth-of-Discharge: DOD = 80%
- Battery Self-Discharge Rate: SD = 0.03%/hr
- Container Farm Size: 2.4m × 2.4m × 12.2m (8ft × 8 ft × 40ft)
- Container Insulation: R = 96.5 W/m^2-K (17 [1/(Btu/hr-ft^2-^{o}F)])
- Heating Efficiency: η = 0.8
- Cooling Energy-Efficiency Ratio (EER) = 3.22 (W_{therm}/W_{AC}) (11 [Btu/hr/W_{AC}])

Appendix A.4. Model Outputs

- Capacity Planning
    - Capacity of solar array [kW]
    - Capacity of battery storage [kWh]
    - Capacity of battery inverter [kW]
- Dispatch Scheduling
    - Time series of solar output [kW]
    - Time series of solar curtailment [kW]
    - Time series of grid purchases [kW]
    - Time series of battery charging/discharging [kW]
    - Time series of demand-side management strategies of specific load [kW]

- Total Energy Output
    - ○ Amount of grid electricity consumed [MWh/yr]
    - ○ Amount of solar electricity generated and curtailed [MWh/yr]
- Total Project Cost Objective
    - ○ Total costs of installing and maintaining solar and storage system
    - ○ Cost of replacing battery storage system in Year 10
    - (a) Total cost of grid electricity purchased

Appendix B. Model Condensed Mathematical Form

Appendix B.1. Decision Variables

- Amount of solar capacity to install *(S)* [kW]
- Amount of battery storage capacity to install *(E)* [kWh]
- Amount of battery inverter capacity to install *(I)* [kW]
- Dispatch time series of battery storage (charge and discharge) *($E_{in/out,t}$)* [kWh]
- Dispatch time series of solar electricity curtailment *(R_t)* [kWh]
- Dispatch time series of grid electricity purchases *(G_t)* [kWh]
- Dispatch time series of heating/cooling system (for Dispatchability Case) *($Q_{heat/cool,t}$)* [kWh]
- Dispatch time series of ventilation system (for Dispatchability Case) *(V_t)* [air changes per hour]
- Dispatch time series of dehumidification (for Dispatchability Case) *(W_t)* [binary]

Appendix B.2. Objective

- Minimize total project costs of container farm energy operations over lifetime:

$$min \sum_{t,y} C_G * G_t + C_S * S + C_E * E + C_I * I + O_S * S + O_E * \ (E_{out,} + E_{in,t}), \quad \text{(A1)}$$

where the summation is over all hourly time steps, t, of a year, y, which are summed over the 20-year lifetime as part of a discounted cash flow.

Appendix B.3. Defined Variables

- Current amount of energy stored in battery storage:

$$SE_{t+1} = SD*[c*E_{in,t} - (1/d)*+E_{out,t}] \quad \text{(A2)}$$

where c and d are the charging and discharging efficiencies, respectively, and the product of which results in a round-trip efficiency of 90%.

Appendix B.4. Constraints

- Overall electricity flows must be balanced in each time step:

$$G_t + S_t + E_{out,t} = l_t + E_{in,t} + R_t \quad \text{(A3)}$$

- Storage state of charge must lie within limits [kWh], given an initial state of charge of 0%:

$$0 < SE_t < DOD*E \quad \text{(A4)}$$

- Battery charging/discharging cannot exceed power requirements of inverter [kW]:

$$0 < E_{in/out,t} < I \tag{A5}$$

- Sensible thermal energy must be balanced at all times:

$$\eta^{*}Q_{heat,t} + Q_{mech,t} = EER^{*}Q_{cool,t} + Q_{vent/inf,t} + Q_{cond,t} + Q_{ET,t} \tag{A6}$$

where $Q_{mech,t}$ is the heat gain of all equipment in time step t; $Q_{cond,t}$ is the heat loss due to conduction through the container envelope; $Q_{vent/inf,t}$ is the heat loss due to ventilation and infiltration; and $Q_{ET,t}$ is the heat loss due to evaporative cooling from plant evapotranspiration (See Appendix C).

- Latent thermal energy must be balanced at all times by balancing moisture flows in the container:

$$L_{ET,t} = L_{dehum,t} + L_{vent/inf,t} \tag{A7}$$

where $L_{ET,t}$ is the moisture, in liters of water, emitted by plants; $L_{dehum,t}$ is the moisture removed by the dehumidifier; and $L_{vent/inf,t}$ is the moisture added or removed via air exchanges with the ambient environment.

Appendix C. Container Farm Energy Modeling

Appendix C.1. Conduction

Heat is transferred via conduction between the interior of the container farm and the ambient environment, through its envelope. Given the Arctic climate, heat is transferred from the container farm interior ($T_{int,t}$) to the cold outdoors ($T_{amb,t}$) during the vast majority of the year. The subsequent heat lost from the container farm (with heat gained from a warm external environment modeled similarly in opposite sign) via conduction is defined as:

$$Q_{cond,t} = (1/R)^{*}A^{*}(T_{int,t} - T_{amb,t}). \tag{A8}$$

The units of heat flows, Q, are in watts of thermal power (W) and, given that the thermal power is an average value over the one-hour time step, is equivalent to amounts of thermal energy in each hour (Wh).

Appendix C.2. Ventilation/Infiltration

Similar to conduction, heat is transferred via convection through ventilated and infiltrated air exchanges between the container farm interior and the ambient environment. At all times, the minimum amount of ventilation coupled with infiltration is assumed to be n = 0.5 air changes per hour (ACH). The subsequent heat lost via convection is:

$$Q_{vent/inf,t} = n^{*}V^{*}c^{*}(T_{int,t} - T_{amb,t}), \tag{A9}$$

where c = 0.335 Wh/m^3-K (1.2 kJ/m^3-K or 0.018 Btu/ft^3-F) is the volumetric heat capacity of air.

The model optimizes additional ventilation by determining the number of forced air changes to perform per hour, accounting for the respective amount of heat loss in Equation (A9). Ventilation is assumed to be performed with existing fan capacity in the container farm with a maximum flow of 60 ACH.

The cost of exhausting CO_2 along with the interior must be accounted for. It is assumed that an optimal level of 900 ppm of CO_2 is maintained in the container farm (approximately 500 ppm above ambient levels) to be absorbed by plants [32]. The cost of CO_2 in compressed cylinders is approximately \$3/kg and given the density of CO_2 equal to 1.98 kg/m^3, the cost of CO_2 per air change is

$0.21. The container farm is assumed not to use CO_2 during the winter (December through February) given operator preference to employ a high degree of ventilation for cooling and dehumidification.

Appendix C.3. Evapotranspiration

The container farm must maintain an optimal humidity level for plant growth; thus, moisture flows must be balanced. In the container farm, moisture is added by plants, removed by a dehumidifier, and either added or removed via ventilation depending on the outdoor humidity level. Each of these components are described below.

Plants emit moisture into the container growing space via evapotranspiration. They absorb water through their roots from the hydroponic growing trays and emit water vapor through openings in their leaves, or stomata. The amount of moisture emitted via evapotranspiration (E) can be determined using the Priestly-Taylor method, assuming that the evaporation rate is energy supply limiting (assuming constant optimal indoor humidity and minimal convection), as defined below with subsequent descriptions of each variable:

$$E = 1.3*E_R*\Delta/(\Delta + \gamma). \quad \text{(A10)}$$

The variable Δ is the saturation vapor pressure gradient (pressure per degree temperature). It is defined as:

$$\Delta = 4098*e_s/(237.3 + T)^2 = 143\ [Pa/^\circ C], \quad \text{(A11)}$$

where e_s is the saturation vapor pressure (2310 Pa at standard conditions) and T is temperature in degrees Celsius.

The value γ is the psychrometric constant given by:

$$\gamma = c_p*p/(0.622*l_v) = 66.6\ [Pa/^\circ C], \quad \text{(A12)}$$

where c_p is the specific heat of air (1005 *J/kg-K*), p is the air pressure (101,000 *Pa* at sea level), and l_v is the latent heat of vaporization ($2.45 * 10^6$ *J/kg* at 20 °*C*).

The variable E_R is the water evaporation rate dictated by an energy-supply limited process defined as:

$$E_R = R_n/(\rho*l_v) = 6.12*10^{-8}\ [m/s], \quad \text{(A13)}$$

where R_n is the net radiation (W/m^2), or total light power (4500 W) per growing area, A, and ρ is the density of water (1000 kg/m^3).

Using Equations (A11)–(A13) into Equation (A10) results in an evaporation rate, E, of plants in the container farm of 5.8 L/hr (5.4×10^{-8} m/s at given volume) when lights are on. This is approximately similar to rated capacities of dehumidifiers in typical container farms. Given the latent heat absorbed to evaporate this much water, this yields 1.3 or 3.9 kWh of evaporative cooling due to plants (Q_{ET}) in each hour, depending on if lights are off or on, respectively, as calculated in Equation (A14):

$$Q_{ET} = E*l_v/(3.6*10^6\ J/kWh). \quad \text{(A14)}$$

In order to meet the specifications of the container farm, a typical dehumidifier rated for such conditions is chosen and uses 1.5 kW of electric power when on and emits 3.2 kW of thermal power (11,000 Btu/hr) when operating [31].

Lastly, the humidity of outdoor air must be accounted for in ventilation and infiltration air flows. The outdoor air in an Arctic climate is typically drier than the interior humidity set point, leading to moisture removal when ambient air replaces indoor humid air. The amount of moisture (in kg of water) lost from the container farm due to replacing indoor air with dry ambient air is modeled in Equation (A15):

$$L_{vent/inf} = H_{in} - \rho*H_{amb,t}*V*ACH_t. \quad \text{(A15)}$$

where H_{in} is the interior humidity ratio setpoint equal to 0.011 kg of water per kg of dry air (equivalent to 70% relative humidity at optimal growing conditions); ρ is the density of air at room conditions (1.2 kg/m^3); $H_{amb,t}$ is the ambient humidity ratio of outdoor air; and ACH is the amount of air changes to perform in each time step.

References

1. Holdmann, G.P.; Wies, R.W.; Vandermeer, J.B. Renewable energy integration in Alaska's remote islanded microgrids: Economic drivers, technical strategies, technological niche development, and policy implications. *Proc. IEEE* **2019**, *107*, 1820–1837. [CrossRef]
2. *Tracking SDG7: The Energy Progress Report (2019)*; The World Bank Group: Washington, DC, USA, 2019.
3. Ma, T.; Yang, H.; Lu, L. Performance evaluation of a stand-alone photovoltaic system on an isolated island in Hong Kong. *Appl. Energy* **2013**, *112*, 663–672. [CrossRef]
4. Jacobson, M.Z.; Delucchi, M.A.; Cameron, M.A.; Coughlin, S.J.; Hay, C.A.; Manogaran, I.P.; Shu, Y.; von Krauland, A.-K. Impacts of green new deal energy plans on grid stability, costs, jobs, health, and climate in 143 countries. *One Earth* **2019**, *1*, 449–463. [CrossRef]
5. Harish, V.S.K.V.; Kumar, A. Demand side management in India: Action plan, policies and regulations. *Renew. Sustain. Energy Rev.* **2014**, *33*, 613–624. [CrossRef]
6. Pina, A.; Silva, C.; Ferrão, P. The impact of demand side management strategies in the penetration of renewable electricity. *Energy* **2012**, *41*, 128–137. [CrossRef]
7. Lovins, A.B. Reliably integrating variable renewables: Moving grid flexibility resources from models to results. *Electr. J.* **2017**, *30*, 58–63. [CrossRef]
8. Snyder, E.H.; Meter, K. Food in the last frontier: Inside alaska's food security challenges and opportunities. *Environment* **2015**, *57*, 19–33. [CrossRef]
9. Bergen, M. *Personal Communication*; Kotzebue Electric Association: Kotzebue, AK, USA, 2020.
10. CropBox: A Farm in a Shipping Container. Available online: https://cropbox.co/ (accessed on 27 July 2020).
11. The Impact of "Plant Factories" on the Electric Grid | Greentech Media. Available online: https://www.greentechmedia.com/articles/read/the-impact-of-plant-factories-on-the-electric-grid (accessed on 11 June 2020).
12. Houtman, J.A. Purdue E-Pubs Design and Plan of a Modified Hydroponic Shipping Container for Research Part of the Agriculture Commons, Art and Design Commons, and the Bioresource and Agricultural Engineering Commons Recommended Citation. Master's Thesis, Purdue University, West Lafayette, IN, USA, 2016.
13. Sparks, R. Mapping and Analyzing Energy Use and Efficiency in a Modified Hydroponic Shipping Container. Master's Thesis, Purdue University, West Lafayette, IN, USA, 2016.
14. Zia, M.F.; Elbouchikhi, E.; Benbouzid, M. Microgrids energy management systems: A critical review on methods, solutions, and prospects. *Appl. Energy* **2018**, *222*, 1033–1055. [CrossRef]
15. Olatomiwa, L.; Mekhilef, S.; Ismail, M.S.; Moghavvemi, M. Energy management strategies in hybrid renewable energy systems: A review. *Renew. Sustain. Energy Rev.* **2016**, *62*, 821–835. [CrossRef]
16. Teichgraeber, H.; Brandt, A.R. Clustering methods to find representative periods for the optimization of energy systems: An initial framework and comparison. *Appl. Energy* **2019**, *239*, 1283–1293. [CrossRef]
17. Hafez, O.; Bhattacharya, K. Optimal planning and design of a renewable energy based supply system for microgrids. *Renew. Energy* **2012**, *45*, 7–15. [CrossRef]
18. Singh, S.; Singh, M.; Kaushik, S.C. Feasibility study of an islanded microgrid in rural area consisting of pv, wind, biomass and battery energy storage system. *Energy Convers. Manag.* **2016**, *128*, 178–190. [CrossRef]
19. Shoeb, M.; Shafiullah, G. Renewable energy integrated islanded microgrid for sustainable irrigation—A bangladesh perspective. *Energies* **2018**, *11*, 1283. [CrossRef]
20. García Tapia, V. Hybrid Renewable Energy System for Controlled Environment Agriculture. Master's Thesis, KTH School of Industrial Engineering and Management, Stockholm, Sweden, 2018.
21. Anderson, K.; Elgqvist, E. *Evaluate Distributed Energy Technologies for Cost Savings and Resilience With REopt Lite Economic Sizing and Dispatch Resilience Evaluation When To Use REopt Lite*; NREL: Golden, CO, USA, 2020.
22. Hale, E.; Stoll, B.; Mai, T. *Capturing the Impact of Storage and Other Flexible Technologies on Electric System Planning*; NREL: Golden, CO, USA, 2016.

23. Neves, D.; Pina, A.; Silva, C.A. Demand response modeling: A comparison between Tools. *Appl. Energy* **2015**, *146*, 288–297. [CrossRef]
24. Neves, D.; Silva, C.A. Optimal electricity dispatch on isolated mini-grids using a demand response strategy for thermal storage backup with genetic algorithms. *Energy* **2015**, *82*, 436–445. [CrossRef]
25. Zhang, S.; Schulman, B. A numerical model for simulating the indoor climate inside the growing chambers of vertical farms with case studies. *Int. J. Environ. Sci. Dev.* **2017**, *8*, 728–735. [CrossRef]
26. Karan, E.; Asadi, S.; Mohtar, R.; Baawain, M. Towards the optimization of sustainable food-energy-water systems: A stochastic approach. *J. Clean. Prod.* **2018**, *171*, 662–674. [CrossRef]
27. Arctic Town Grows Fresh Produce in Shipping Container Vertical Garden. Available online: https://inhabitat.com/agtech-start-up-plenty-plans-to-grow-hydroponic-peaches/ (accessed on 11 June 2020).
28. Sæterbø, M. *Arctic Agriculture by Using Fish Farming Waste in Northern Norway*; UiT Norges arktiske universitet: Tromso, Norway, 2019.
29. Bos-Jabbar, T. *Personal Communication*; ColdAcre Food Systems: Yukon, BC, Canada, 2020.
30. Trane Technologies Inc. Engineers Newsletter Providing Insights for Today's Hvac System Designer Volume 48-3 Indoor Agriculture: HVAC System Design Considerations. Available online: https://www.trane.tm/content/dam/Trane/Commercial/global/products-systems/education-training/engineers-newsletters/airside-design/admapn071en-082019.pdf (accessed on 20 June 2020).
31. Commercial Dehumidifiers | Industrial Dehumidifiers | Quest. Available online: https://www.questclimate.com/ (accessed on 28 June 2020).
32. Carbon Dioxide in Greenhouses. Available online: http://www.omafra.gov.on.ca/english/crops/facts/00-077.htm (accessed on 25 June 2020).
33. Hachem-vermette, C.; Dara, C.; Kane, R. Towards net zero energy modular housing: A case study. *Modul. Offsite Constr. Summit Proc.* **2018**. [CrossRef]
34. Alaska Energy Authority. *Personal Communication*; Alaska Energy Authority: Anchorage, AK, USA, 2020.